

CHARACTERIZATION AND DELINEATION OF PLUMES, CLOUDS AND FIRES IN AN AVIRIS IMAGE

Michael K. Griffin,¹ Su May Hsu, Hsiao-hua K. Burke and J. William Snow
MIT Lincoln Laboratory, Lexington, MA 02420

1. INTRODUCTION

Hyperspectral imaging (HSI) sensors have been used for more than a decade to aid in the detection and identification of diverse surface targets, topographical and geological features. HSI data provides a scene analyst with a wealth of spectral (100s of channels) and spatial (10s of meters) information. Techniques for scene characterization can utilize individual or combinations of spectral bands to identify specific features in an image. Processing of the entire spectral domain (e.g., through principal components analysis) can also be used to reduce the dimensionality of hyperspectral data as well as to facilitate spectral feature extraction and material identification.

This paper deals primarily with the problem of characterization of a partially smoke- or cloud-filled atmosphere. Proper analysis of the scene allows further sensing of underlying surface features such as actively burning and burn scarred regions. Both a physics-based and a semi-automated feature extraction approach are used for identifying and characterizing features in a set of AVIRIS scenes dominated by areas of smoke plumes, clouds and burning grassland as well as burnt vegetation. In the physics-based approach, natural occurring water clouds are contrasted with smoke plumes, burn scarred land is extracted using an NDVI-like index formula and active or smoldering fires are identified with enhanced NIR/SWIR signatures. New smoke plumes (smaller particles and optically thicker) are discriminated from old plumes (larger particles and optically thin) by spectral differences in the visible and SWIR.

In contrast to the physics-based approach, a semi-automated principal components analysis (PCA) technique is applied to the same images and a scene classification is done. This approach utilizes the diversity of the full² set of spectral information to derive aspects of the relative signal variance of specific features in a scene. Using appropriate thresholds on the component images, scene features can be separated. However, the PCA technique has no ability to identify a feature. A combination of the two approaches is used to both discriminate (PCA) and classify (physics based) various features in a smoke/cloud filled scene. The following sections provide a brief description of the hyperspectral data source (AVIRIS), the two atmospheric characterization techniques and a comparison of the individual results for three different fire scenes.

2. AVIRIS HYPERSPECTRAL SENSOR

The Airborne Visible-InfraRed Imaging Spectrometer (AVIRIS) sensor has been used extensively to provide measurements in the visible, near- and shortwave-infrared spectrum. AVIRIS contains 224 different detectors, each with a spectral bandwidth of approximately 10 nanometers (nm), allowing it to cover the entire range between 380 nm and 2500 nm. AVIRIS uses a scanning mirror to sweep back and forth in a whisk broom fashion, producing 614 pixels for each scan. Each pixel produced by the instrument covers a 20x20 meter square area on the ground (with some overlap between pixels), yielding a ground swath width of approximately 10 kilometers for an ER-2 flight altitude of 20 km (see Vane, 1987 and Vane, et al., 1984 for more information on AVIRIS). AVIRIS measurements are distributed in units of radiance. All algorithms described below operate on apparent reflectance which is obtained by converting the radiance to reflectance using the known solar zenith angle and the top-of-the-atmosphere solar irradiance for each AVIRIS channel.

The AVIRIS scene chosen for initial testing of the two algorithms was collected in the foothills east of Linden, CA on 20 August 1992 (Gao, et al., 1993). The scene consists of a grass fire producing a thick plume of smoke towards the east (see Fig. 1a). A cloud produced most likely by the thermal properties of the fire overlies the smoke plume. Towards the northwest, two smoldering fires are produce a thin veil of smoke that covers much of

¹ Voice: 781-981-0396; Fax: 781-981-7271; Email: griffin@ll.mit.edu

² In this study, the PCA utilizes approximately 130 of the 224 AVIRIS bands. Channels located in the water vapor absorption bands were not used in the computations.

the upper half of the scene. The southwest portion of the scene is cloud and smoke free; a golf course, lake, roads and rivers can be identified. Small shadows are also observed just to the north of the cloud. This scene (identified as the Linden scene in this paper) provides a variety of atmospheric and surface features from which to orient and characterize. A plot of the spectral characteristics of various identified features in the scene is shown in Fig. 1b.

Two other scenes were also used to test the algorithms: 1) a rural scene with a small fire and associated smoke plume (Rice Field scene) collected on 8 August 1994 near Stockton, CA (Fig. 2a) and 2) a large fire and smoke plume associated with rainforest clearing near Cuiaba, Brazil on 25 August 1995 (Fig. 2b), collected as part of the Smoke, Cloud, Aerosol and Radiation experiment (SCAR-B scene; Green, 1996).

3. PRINCIPAL COMPONENT ANALYSIS (PCA)

To reduce the HSI data dimensionality and therefore the computational complexity, feature extraction can be performed on the spectral data before application of image pixel clustering. Principal component analysis is generally used to de-correlate data and maximize the information content in a reduced number of features (Richards, 1994; Geladi and Grahn, 1997). The covariance matrix is first computed over the pixel spectra contained in the HSI data cube of interest. Eigenvalues and eigenvectors are then obtained for the covariance matrix Σ as given below:

$$\Sigma = E \{ (X - X_m)(X - X_m)^T \} = \Phi \Lambda \Phi^T$$

where, X represents the spectral vector data; X_m the mean spectral vector over the data cube and E the average operator over the entire data cube. Φ is a matrix consisting of columns of eigenvectors and Λ is a diagonal matrix of eigenvalues.

Using the eigenvectors as a new coordinate system, the HSI data cube is then transformed into principal components, also called eigenimages. The eigenimages associated with large eigenvalues contain most of the information while the eigenimages associated with small eigenvalues are noise-dominated. Thus principal component transform allows determination of the inherent dimensionality and segregation of noise components of the HSI data. The components are ranked in descending order of the eigenvalues (image variances). Since backgrounds constitute the majority of information in the scene, they are contained in the first few principal components. Anomalies, which comprise only a small fraction of the scene, are in higher numbered principal components. Figure 3 displays the 1st, 2nd and 5th principal components of the AVIRIS data for the Linden Scene. The first component shows the overall intensities of features such as bright clouds and smoke plumes over backgrounds. A dark area which appears to be the source of the thick smoke is apparent in the 2nd component. In the 5th component, a small fraction of the image pixels are in contrast to the image backgrounds.

3.1 Classification with PCA

It is apparent in the PCA above that the first two principal components of the Linden AVIRIS data contain background information and the 5th component shows an anomaly. A classification can be obtained from these components. Since the principal components are orthogonal and thus de-correlated, different image features can be separated from the components with appropriate thresholds. Figure 4 depicts the histogram of pixel distribution as a function of values in the 1st principal component. The peaks and valleys in the histogram are due to several groups of image features at different intensity levels. These can be separated with thresholds of -22000, -13200, -4900 and 19600 at the histogram valleys as shown below:

	Shadow	< -22000
-22000 <	Clear	< -13200
-13200 <	Smoke (large particle)	< -4900
-4900 <	Smoke (small particle)	< 19600
19600 <	Cloud	

The hot pixels are less than -5000 in the second component; and the anomalies are less than -9000 in the 5th component. The resulting classification is shown in Figure 5.

The mean class spectra of the seven classes are plotted in Figure 6. The cloud is significantly brighter than the smoke over the entire spectral region. The hot area is brightest in the spectral region 2000 to 2500 nm, while the fire pixels are bright for wavelengths greater than 1150 nm. A small dip at 700 nm followed by a rise at 740 nm in the spectrum of large particle smoke indicates its partial transparency to the vegetative background.

4. PHYSICS-BASED ANALYSIS

Utilizing the diverse spectral and spatial information afforded by HSI observations of a scene, formulas can be developed relating the measurements in various channels to discriminate specific features in a scene (i.e., clouds, smoke, lakes, etc.). In an effort to characterize the features in the Linden scene, empirical formulas were developed based upon spectral characteristics of each feature. Equations for the discrimination of clouds, large and small particle smoke, high temperature surface regions and areas of burnt vegetation have been derived. A brief description of each equation follows. Ultimately, these formulas can be used to classify regions identified by the PCA routine as having similar properties.

4.1 Clouds

Clouds are typically the brightest feature in an AVIRIS image. The reflectance from clouds is nearly invariant in the visible and near-IR window regions, since the size of the scatterers in the cloud are much larger (size parameter $\gg 1$) than the sensor wavelengths. This is in contrast to atmospheric aerosols whose particle size tends to be at or near the observed wavelengths of radiation and therefore the scattering effects vary significantly with wavelength throughout the visible and near-IR. This information can be used to discriminate clouds from darker background objects and from bright but spectrally variable smoke plumes and fires.

A three step approach is used to isolate clouds in an AVIRIS scene. The first step removes dark background objects such as rivers, lakes and vegetation from consideration by applying a threshold to the 640 nm reflectance image. A threshold of 0.20 has been observed to eliminate a large portion of the background scene. The second step takes advantage of the spectral invariability of cloud. A ratio of the 640 and 860 nm reflectance images is obtained and all pixels with ratios less than 0.70 are eliminated. This value is derived from the technique used on AVHRR data to discriminate cloud regions (Gustafson, 1994). It has the effect of removing much of the smoke and vegetation that display distinct changes over the range of frequencies from 640 to 860 nm. Finally, to isolate the cloud from the surrounding thick smoke, a channel in the 1600 nm window region is used. At these wavelengths, the atmosphere is nearly transparent to the affects of smoke particles while the large cloud particles still provide strong reflectance. A threshold of 0.35 was obtained from observation of the spectral characteristics in this region. Those remaining pixels with reflectance values above 0.35 were designated cloud.

4.2 Hot Spots

Areas of active burning or smoldering fires have distinct spectral characteristics of their own. Figure 1b shows the effect high surface temperatures have on the measured radiance. Both the curves representative of the hot area and active fire display gradually increasing radiance (reflectance) in the SWIR region. Non-physical reflectances greater than one in this figure are an indication of a combination of both solar and a significant thermal component to the measured radiance. A high surface temperature (> 400 K) is needed to produce a significant thermal component at these wavelengths (Green, 1996). Reflectance differences greater than 0.1 between channels in the SWIR (2200 nm) and the NIR (1095 nm) allowed the discrimination of these features.

The intensity of a fire, designated by its effective surface temperature, can be a useful product to forestry and land management programs. While active burning areas are relatively easy to identify in AVIRIS imagery by their spectral signature in the SWIR, a separation of the solar and thermal components must be done before an estimate of the surface temperature of the fire can be obtained. The problem here is the lack of knowledge of the surface reflectance characteristics of the terrain surrounding the fire which are needed to estimate the solar component to the signal (Green, 1996). A simple method to derive a value for the *minimum* surface temperature of the fire is the assumption that the reflected solar component be equivalent to the incident solar radiance. This is equivalent to assuming that the atmosphere is non-absorbing and non-scattering (a transmission of one) and the surface is a perfect reflector. While this may greatly underestimate the fire intensity, it does provide a lower boundary on this parameter. With more knowledge about the scene (atmospheric transmission or upwelling path

radiance), a more accurate estimation of the fire intensity could be obtained even without knowledge of the surface reflectance characteristics.

4.3 Smoke plumes

As described in Section 4.1 above, the reflectance characteristics of smoke plumes vary systematically with wavelength. Also, smoke from smoldering fires may contain larger particles than that from more intense fires; the particles have had more time to coagulate. Therefore, it is useful to separate the smoke category into two subcategories: large and small particle smoke. In the Linden scene, small particle smoke is produced by the main fire near the center of the scene and is quite opaque in the visible and near-IR wavelengths. Observations of the spectral signature of small particle smoke indicate that a comparison of visible and SWIR channels provide a method of discrimination. When the difference between the reflectances at 490 nm and 2200 nm is greater than 0.02, small particle smoke is indicated.

Large particle smoke, observed as the large thin plume emanating from the two small fires in the upper left of the Linden scene, is relatively transparent to observations in the visible and near-IR. An empirical relationship was derived using visible channels only to isolate areas with large particle smoke. When the reflectance at 430 nm is greater than 0.18 and the ratio of the reflectance at 430 and 510 is greater than 1.2, then large particle smoke is indicated.

4.4 Burn Index

Biomass burning not only produces detectable smoke plumes but results in burn scars having spectral signatures that are distinct from that of undisturbed vegetation. Areas of burnt vegetation display relatively low reflectances especially in the 700 to 900 nm band where normal undisturbed vegetation displays a reflectance maximum. Vegetation indices have been developed which highlight the change from low to high reflectance in the visible and near-IR spectral region. The Normalized Difference Vegetation Index (NDVI) is commonly used to discriminate various surface vegetation features. The NDVI cannot be used under cloudy or smoky conditions since both tend to mask the underlying signal at these wavelengths. In an effort to obtain information about the spatial extent of biomass burning, a burn index (BI) was devised that can be used to detect areas of burnt vegetation using wavelengths that are more transparent to smoke. The formula used here for burn scar detection is

$$BI = \frac{\rho_{1100} - \rho_{2200}}{\rho_{1100} + \rho_{2200}}$$

where ρ_n represents the reflectance at a wavelength of n nanometers. Before application of the BI, a cloud and thick smoke mask is applied to the scene. Figure 7 shows the result of application of the BI to the Linden scene. A large burn scar is observed under the thin smoke plume in the upper left quadrant of the image.

5. COMPARISON OF RESULTS

Figure 8 displays the results from application of the above two techniques to the Linden scene. Figure 8b represents a composite of the results from applying the above formulas to the AVIRIS data. Features identified in Fig. 8b were matched to classes derived from application of the PCA technique to the Linden scene and are shown in Fig. 8a. Two classes for which formulas have not been derived (visually identified as fire and shadow) are indicated in the PCA composite. Both techniques seem to provide good individual characterizations of the Linden scene, even to the differentiation of large particle (darker magenta) and small particle (lighter magenta) smoke.

Figure 9 provides results from the Rice Field scene. The observed smoke plume and originating fires are identified by both techniques. The physics-base approach seems to detect more of the outlying parts of the smoke plume than the PCA technique, however, the shape of the detected areas has a certain angled appearance indicative of the rectangular nature of the underlying background. The PCA detected smoke plume has a more realistic plume-like shape. The difficulty with this scene is the diversity of the background reflectance. A large range of reflectance features corresponding to various seasonal agricultural crops, urban areas, rivers, a canal, and roads provide a highly variable background from which to apply the algorithms.

In the SCAR-B scene shown in Fig. 10, the PCA technique detects both large and small particle smoke while the physics based technique only detects large particle smoke. It is possible that a range of smoke particle sizes exist within the smoke plume, but it appears that the discrimination is based more on opacity of the smoke than on the effect of particle size. What appears to be cloud in the bottom right corner of the image is detected by both routines. Hot spot areas are shown in the lower right corner indicative of the origin of the smoke plume and the location of the actively burning fires. The underlying vegetation is quite dark and provides little indication of the surface topography.

6. SUMMARY

Two techniques for characterization of atmospheric features were applied to three AVIRIS scenes. A technique based upon principal components analysis was used to separate distinct feature classes in an AVIRIS image. The PCA does not provide information on the identity of the resultant classes, only that they are distinguished in the analysis of the image. To identify these features, a physics based approach which utilizes the unique characteristics of the spectral signatures of the features is applied. Results are matched with the PCA classes to provide feature identification. The techniques were applied separately to three AVIRIS scenes. The techniques were in agreement as to separation of classes and the general shape of the observed features for the two California scenes. The SCAR-B scene showed a discrepancy in the depiction of the smoke plume. The PCA detected two separate classes for the smoke plume while the physics based technique only found one type of smoke. It is likely that the PCA result was in part influenced by the change in opacity and/or visible brightness of the smoke plume as the classes tend to follow contours associated with these phenomena. With some improvement to the algorithms, indications are that the combination of the two techniques with the inclusion of the burn index, could provide a useful technique for the characterization and identification of scenes containing clouds, smoke and active fires from HSI data.

7. REFERENCES

- Gao, B.-C., Y. Kaufman and R. Green, 1993: Remote Sensing of Smoke, Clouds and Fire Using AVIRIS Data. *Proc. of the Fifth Annual JPL Airborne GeoScience Workshop*, JPL Publication 93-16, Pasadena, CA, 61-64.
- Geladi, P. and H. Grahn, 1997: *Multivariate Image Analysis*. John Wiley & Sons.
- Green, R., 1996: Estimation of Biomass Fire Temperature and Areal Extent from Calibrated AVIRIS Spectra. *Proc. of the Seventh Annual JPL Airborne GeoScience Workshop*, JPL Publication 96-16, Pasadena, CA, 105-113.
- Gustafson, et al., 1994: Support of Environmental Requirements for Cloud Analysis and Archive (SERCAA): Algorithm Descriptions. *Scientific Report #2*, PL-TR-94-2114, Phillips Laboratory, Hanscom AFB, MA, 108p.
- Richards, J., 1994: *Remote Sensing Digital Image Analysis*. Springer-Verlag, 133 p.
- Vane, G., 1987: Airborne Visible/Infrared Imaging Spectrometer (AVIRIS). *JPL Publication 87-38*, 97 p.
- Vane, G, M. Chrisp, H. Enmark, S. Macenka and J. Solomon, 1984: Airborne Visible/Infrared Imaging Spectrometer: An advanced tool for earth remote sensing. *Proc. 1984 IEEE Int'l Geosc. & Rem. Sens. Symp.*, SP215, 751-757.

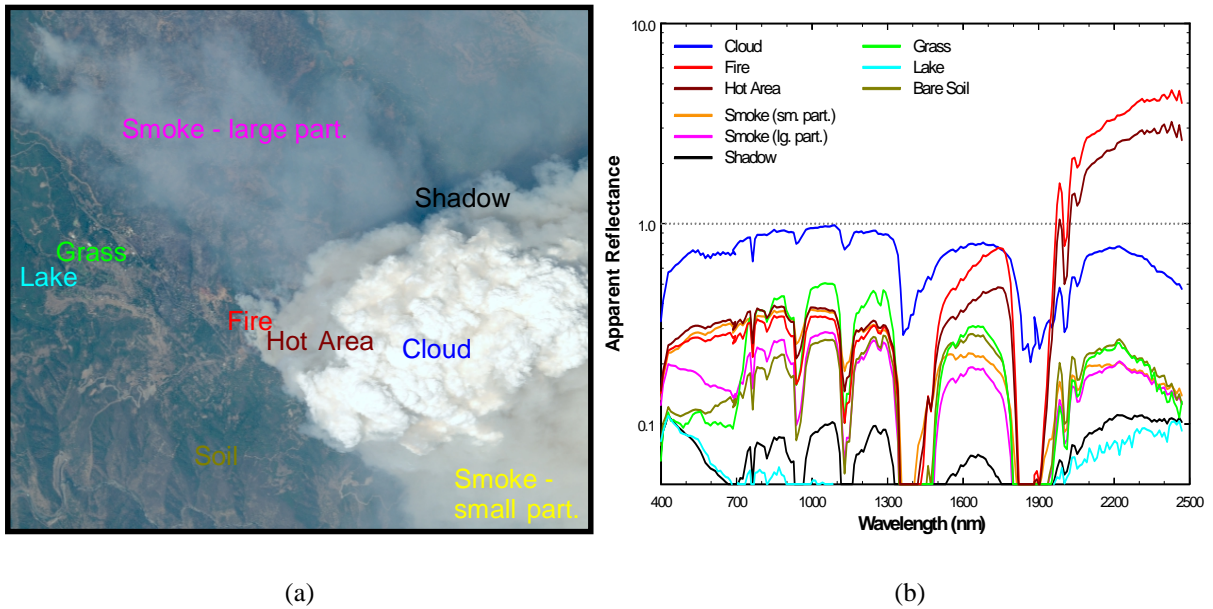


Figure 1. a) AVIRIS RGB image for the Linden, CA scene collected on 20-Aug-1992, denoting location of various features of interest and b) a plot of the spectral distribution of the apparent reflectance for those features.

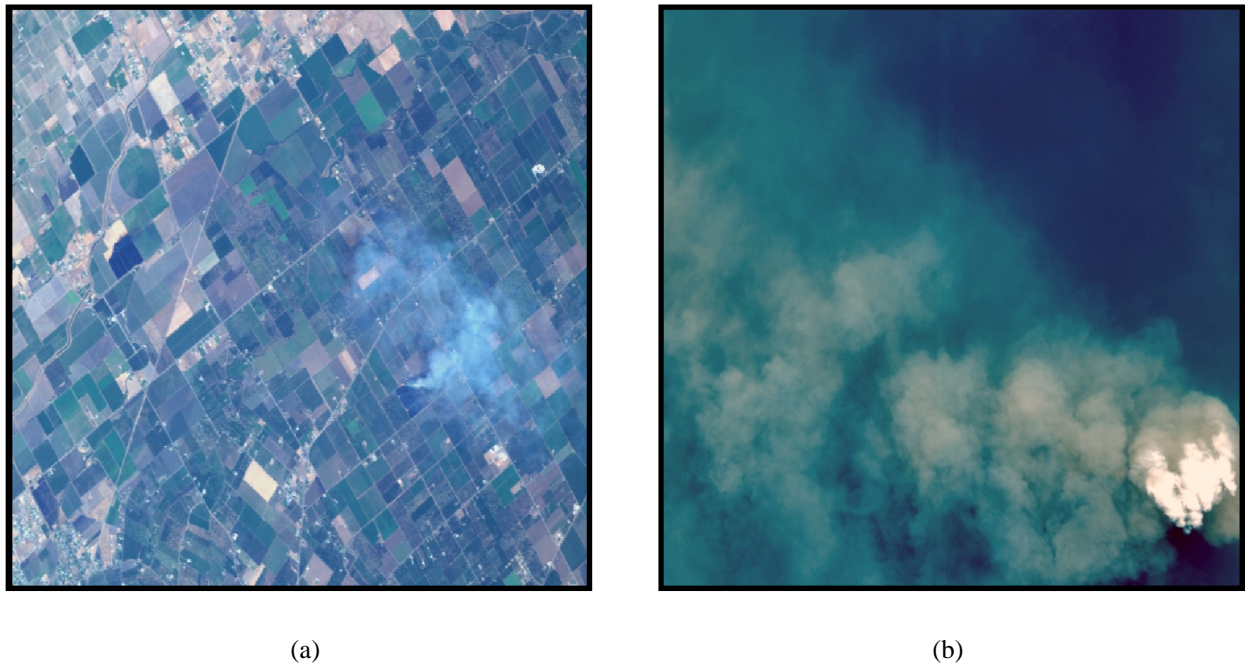


Figure 2. AVIRIS RGB images of a) a rice field fire in California on 9-Aug-1994 and b) a rainforest fire near Cuiaba, Brazil on 25-Aug-1995.

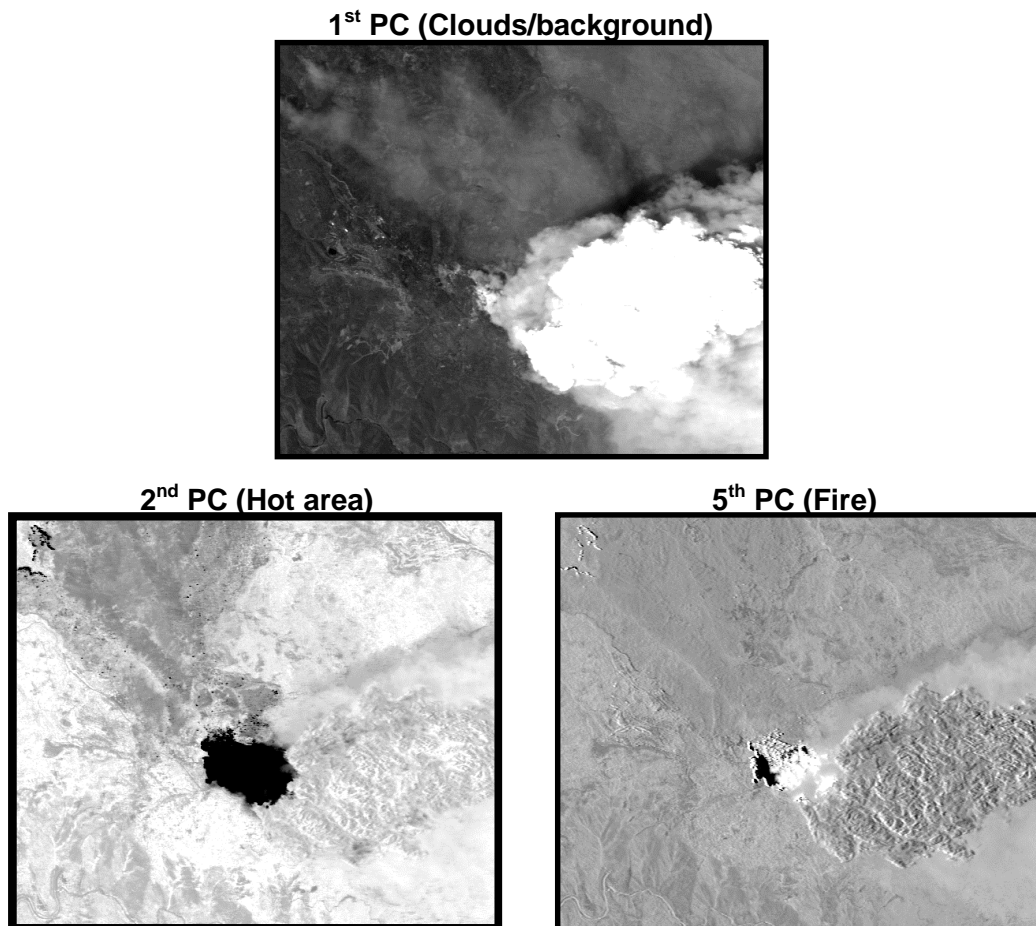


Figure 3. The 1st, 2nd and 5th principal components of AVIRIS data for the Linden scene.

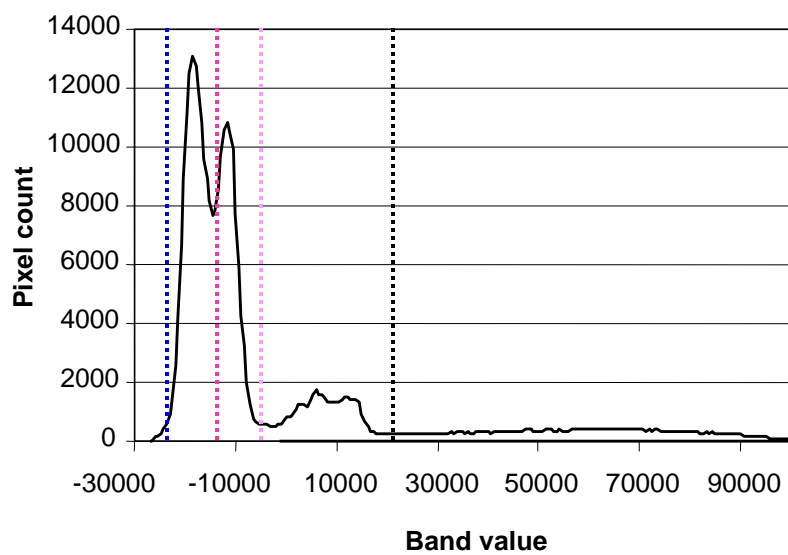


Figure 4. Histogram of pixel distribution as a function of values in the 1st principal component.

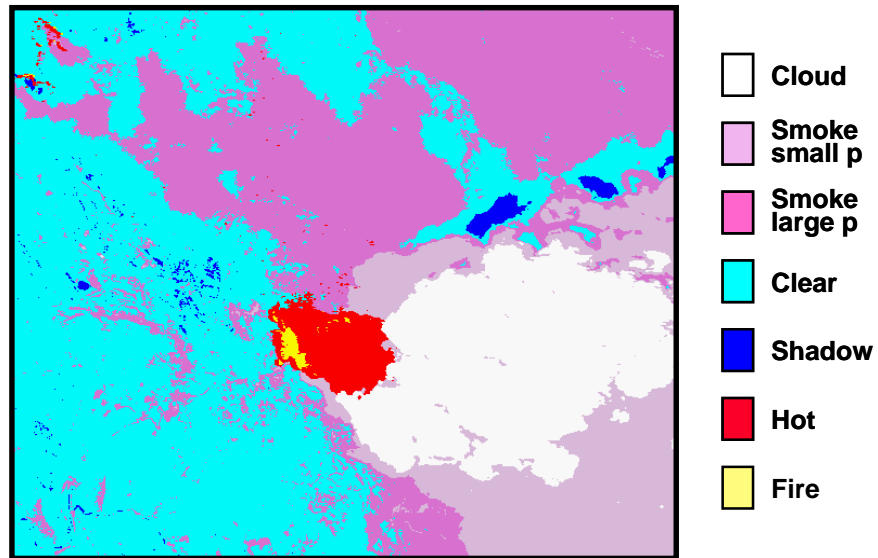


Figure 5. Classification using the 1st, 2nd and 5th principal components.

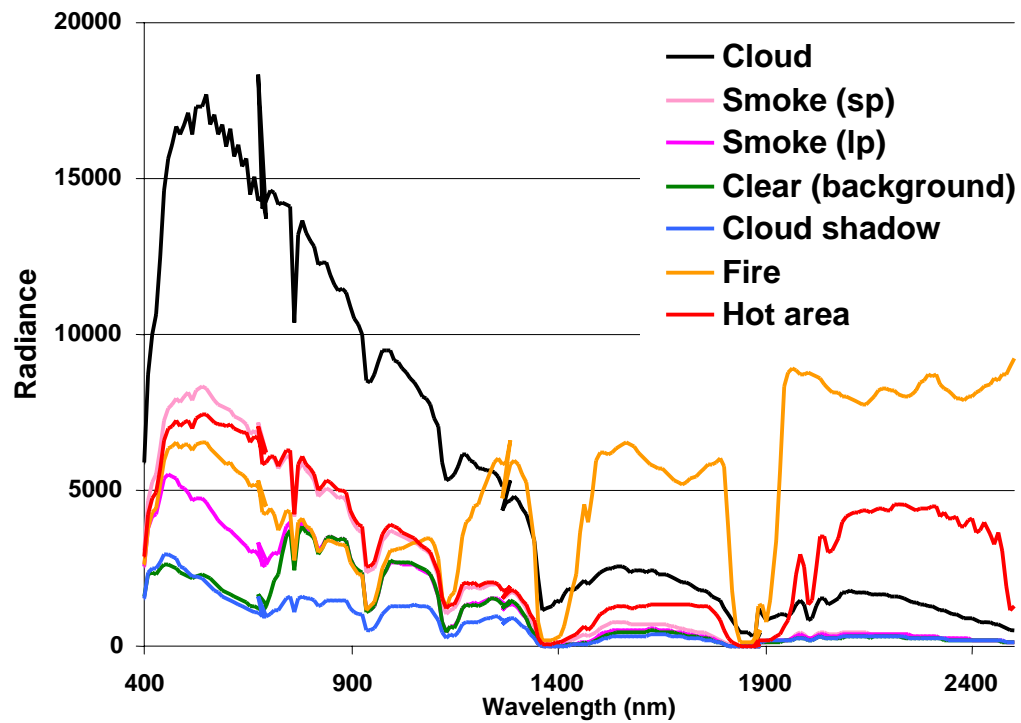


Figure 6. Mean spectra of seven classes in the classification using three principal components.

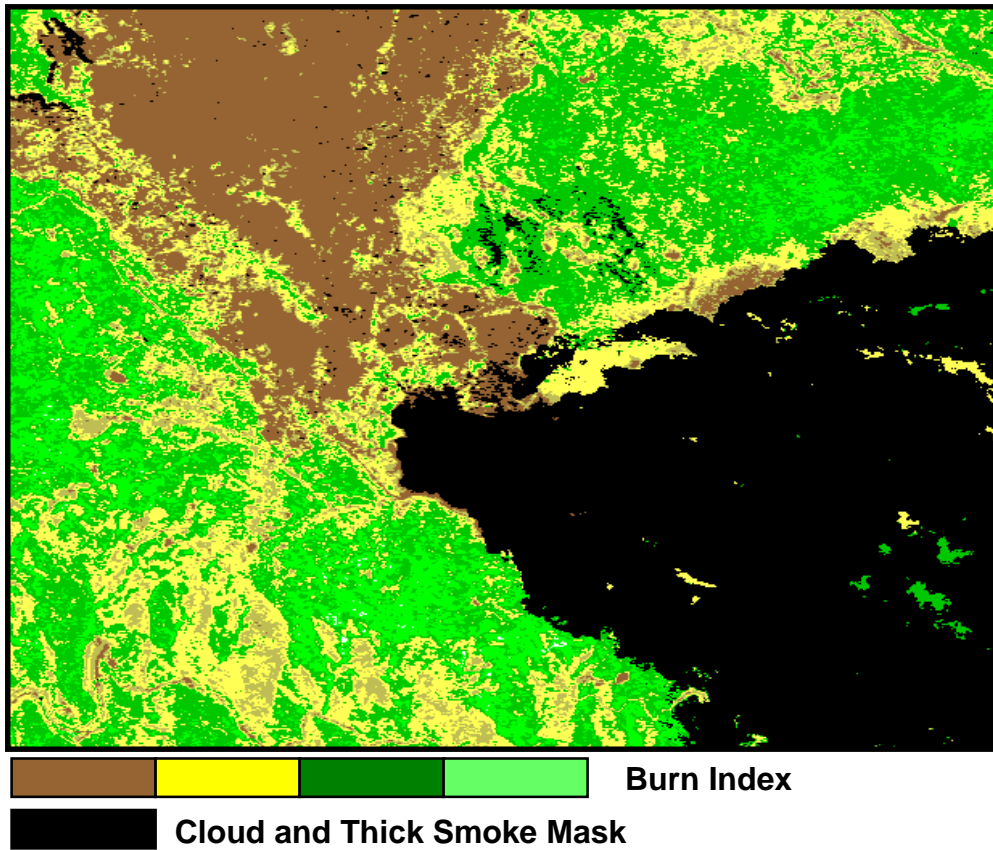


Figure 7. Application of the Burn Index to the Linden AVIRIS scene. Brown areas in upper left quadrant are indicative of burn scars. Cloud and thick smoke regions have been masked out (black).

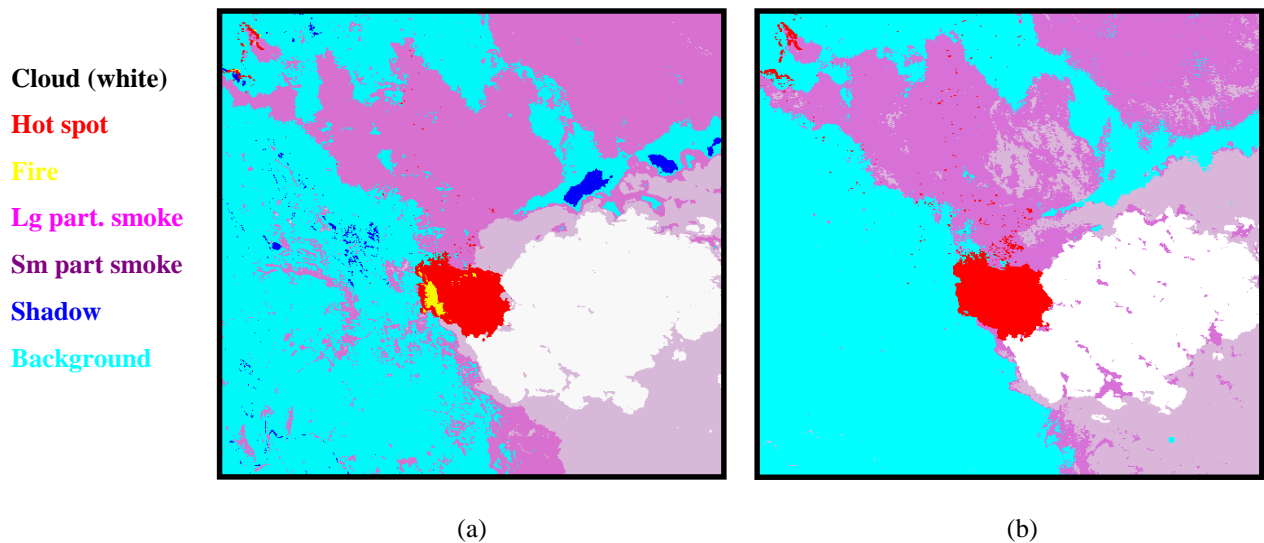
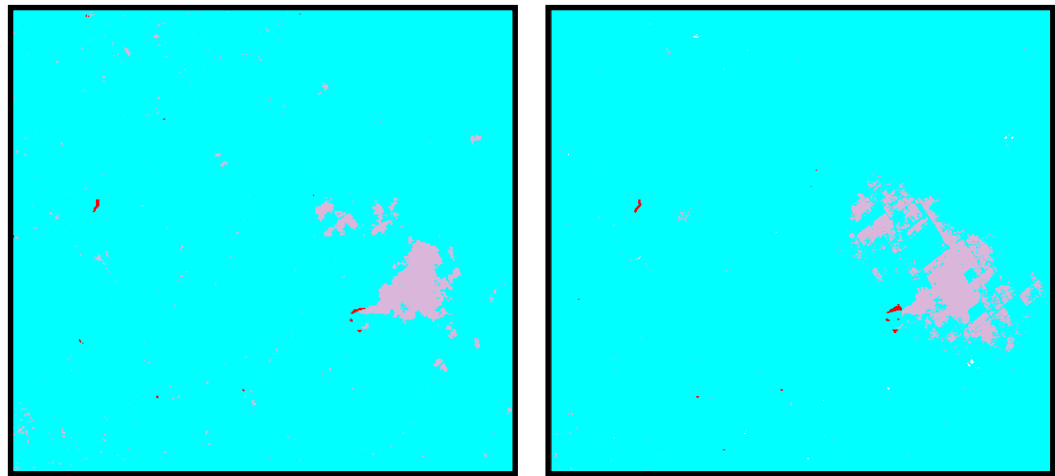


Figure 8. Composite results of the image characterization for the Linden AVIRIS image from a) PCA and b) physics based techniques.

Hot spot
Sm part smoke
Background

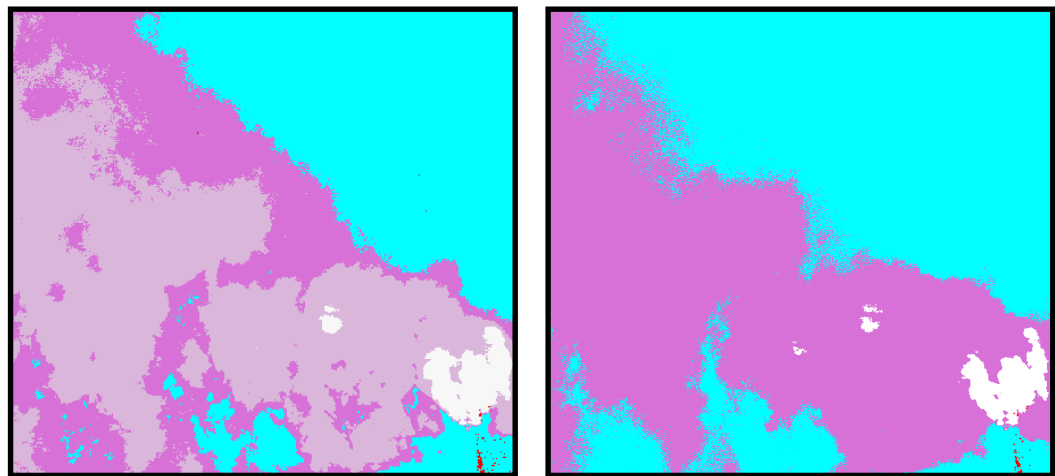


(a)

(b)

Figure 9. Composite results of the image characterization for the Rice Field AVIRIS image from a) PCA and b) physics based techniques.

Cloud (white)
Hot spot
Lg part. smoke
Sm part smoke
Background



(a)

(b)

Figure 10. Composite results of the image characterization for the SCAR-B AVIRIS image from a) PCA and b) physics based techniques.